

## Incorporating Radiation Effects into Edge Plasma Transport Models with Extended Atomic Data Tables

H. A. Scott, M.L. Adams

*Lawrence Livermore National Laboratory, Livermore, CA, USA*

Plasmas at the tokamak edge can be very optically thick to hydrogen resonance lines. The resulting strong line radiation can significantly affect the ionization and energy balance in these plasmas. One method of account for effects is to self-consistently couple a partially ionized plasma transport model with a nonlocal thermodynamic equilibrium (NLTE) model incorporating line radiation transfer. This approach has been implemented in one dimension [1], but would be computationally challenging and expensive to implement in multiple dimensions. Approximate treatments of radiation transfer can decrease the computational time, but would still require coupling to a multidimensional plasma transport model to address realistic geometries, e.g. the tokamak divertor. Here, we consider the development of atomic hydrogen data tables that include radiation interactions and can be easily applied to multidimensional geometries.

The atomic hydrogen data tables currently used in edge plasma codes are constructed under the assumption that line radiation can freely escape, i.e. the optically thin approximation. The optically thin regime is convenient for tabulation, as the necessary data – ionization/recombination rates, cooling rates and excited state fractions – depend only on the electron density and temperature. However, this assumption fails in the high density, low temperature regimes prevalent in detached tokamak divertors. The effects of radiation increase with size and, under the conditions expected for the ITER divertor, can drastically alter the atomic rates, affecting plasma transport and energy balance. This is reflected in the plasma profiles in the divertor region, as well as in the incident heat flux on the divertor target plate.

A series of 1D divertor simulations, discussed in detail in [2], helps to quantify the radiation effects. An important engineering constraint in tokamaks is the peak divertor target plate incident heat flux,  $q_{\text{out}}$ . Table 1 summarizes the effect of hydrogen resonance line radiation on this parameter by comparing the amount of heat flux on the divertor target plate with the total radiative heat flux escaping the divertor region,  $q_r$ , where both heat fluxes are expressed as fractions of the total heat flux entering the divertor region. The values labelled

“thin” assume an optically thin plasma while those labelled “full” reflect a full treatment of radiation transfer. Radiation effects increase the incident heat flux on the divertor target plate by more than a factor of 2.

The radiation field at a particular position depends not only on local conditions, but also on the plasma profiles and geometry. However, we have chosen to parameterize the radiation effects through a single additional parameter,  $\tau$ , defined by

$$\tau = \int_0^s 10^{14} n_n(s') ds'$$

where  $n_n$  is the neutral ground state number density and the integration path extends from the point under consideration to the plasma boundary.  $\tau$  is proportional to the Lyman  $\alpha$  optical depth, and is numerically close to that quantity for a hydrogen plasma with a temperature of order 1 eV. This parameterization utilizes the dominant character of Lyman  $\alpha$  radiation in partially ionized hydrogen plasmas.

	$q_r$	$q_{out}$
thin	-0.805	+0.195
full	-0.555	+0.445
$\tau_{min}$	-0.537	+0.463
$\tau_{eff}$	-0.477	+0.523
$p_{escape}$	-0.486	+0.514

Table 1

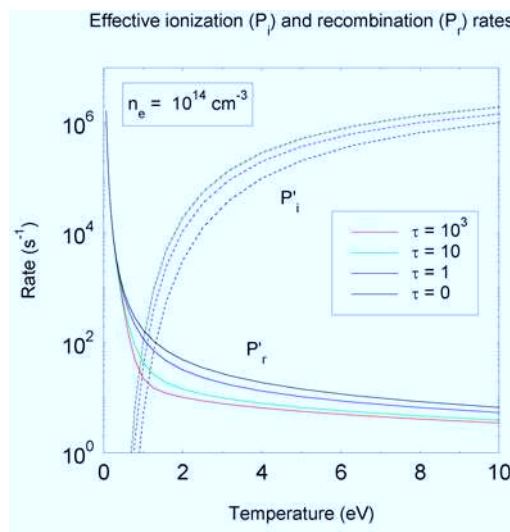


Fig. 1

For a given value of  $\tau$ , the extended tables include rates and excited state fractions calculated for conditions at the center of a uniform plasma slab of width  $2\tau$ . Figure 1 displays the (effective) ionization ( $P_i$ ) and recombination ( $P_r$ ) rates as a function of temperature for an electron density of  $10^{14} \text{ cm}^{-3}$  and several values of  $\tau$ . (For a full definition and derivation of these quantities, see [2]). The rates depend strongly on both temperature and  $\tau$  in this regime. Figures 2 and 3 display the ionization rates and excited state fraction coefficients (for the  $n=3$  state) as a function of  $\tau$  for a few temperatures. The choice of  $\tau$  as the additional

parameter allows for accurate interpolation, while the range included in the tables runs from the coronal (low  $\tau$ ) regime to the LTE (high  $\tau$ ) regime.

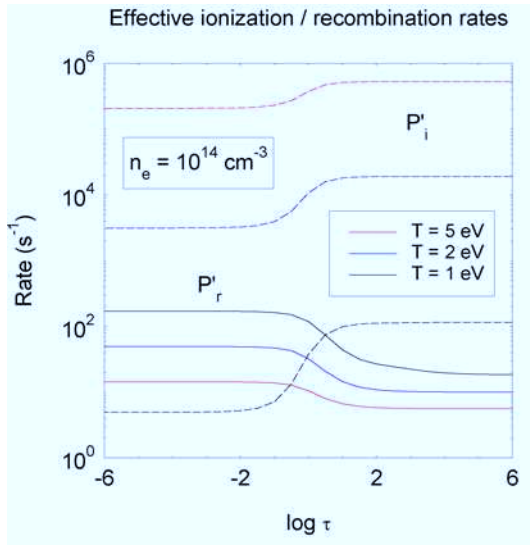


Fig. 2

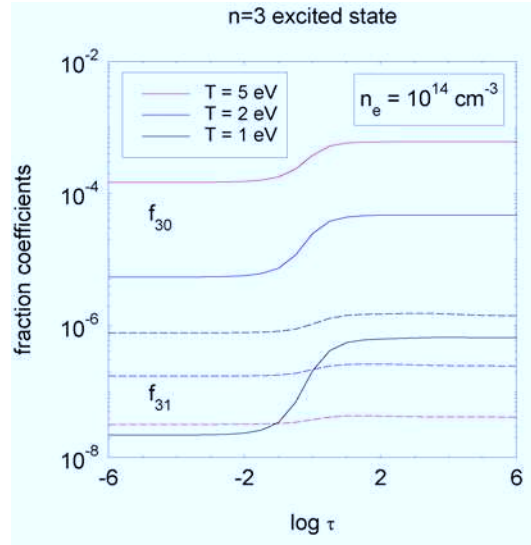


Fig. 3

While these tables have been constructed for a specific geometry, we can apply them in more general situations by using an appropriate value of  $\tau$  as the lookup value. Focusing on Lyman  $\alpha$ , the single parameter affecting the atomic rates is the escape probability  $p$ , which can be related to the optical depth  $\tau$  in a given direction via the simple formula:

$$p = \frac{1}{1 + \frac{15\tau}{\sqrt{T_e[\text{eV}]}}} \Leftrightarrow \tau = \frac{\sqrt{T_e[\text{eV}]} \left( \frac{1}{p} - 1 \right)}{15}$$

This approximate relationship holds with sufficient accuracy in the transition region of moderate values of  $\tau$ , even though it is incorrect in the asymptotic limit of large  $\tau$ . Given this relationship, the appropriate value of  $\tau$  is then obtained by averaging  $p$  over solid angle and inverting the above relationship.

The results of simulations using these data tables in place of the radiation transfer treatment are also included in Table 1. The values labelled “ $\tau_{\text{min}}$ “ use  $\tau$  calculated from the minimum distance to a boundary, while those labelled “ $\tau_{\text{eff}}$ “ use  $\tau$  obtained from the above prescription, incorporating distances to both boundaries. Both methods reflect large radiation effects and either is vastly preferable to ignoring these effects. The  $\tau_{\text{min}}$  values are fortuitously close to those from the full treatment through cancellation of errors in the geometric treatment and in the assumption of homogeneity implicit in the tabular treatment.

The values labelled “ $p_{\text{escape}}$ ” were calculated with an escape factor radiation treatment using the full geometry but assuming homogeneity and the results are quite close to the  $\tau_{\text{eff}}$  values. For 2D or 3D geometries, one further modification is necessitated by the fact that the tables were constructed from planar geometry. Dividing the final value of  $\tau$  by 4 compensates for this and produces values close to those obtained from detailed calculations. Figure 6 shows the ionization rate obtained from (a) radiation transfer calculations, (b) table lookups using  $\tau_{\text{eff}}$  and (c) table lookups using  $\tau_{\text{min}}$ , for a 2D plasma configuration. The test geometry measures 1 cm horizontally, corresponding to optical depth  $\sim 4$  for Lyman  $\alpha$ , and 20 cm vertically, with  $n_n=n_e=10^{14} \text{ cm}^{-3}$  and  $T=2 \text{ eV}$ . The prescription for  $\tau_{\text{eff}}$ , reflects the geometric effects much better than  $\tau_{\text{min}}$  and does very well at reproducing the detailed results.

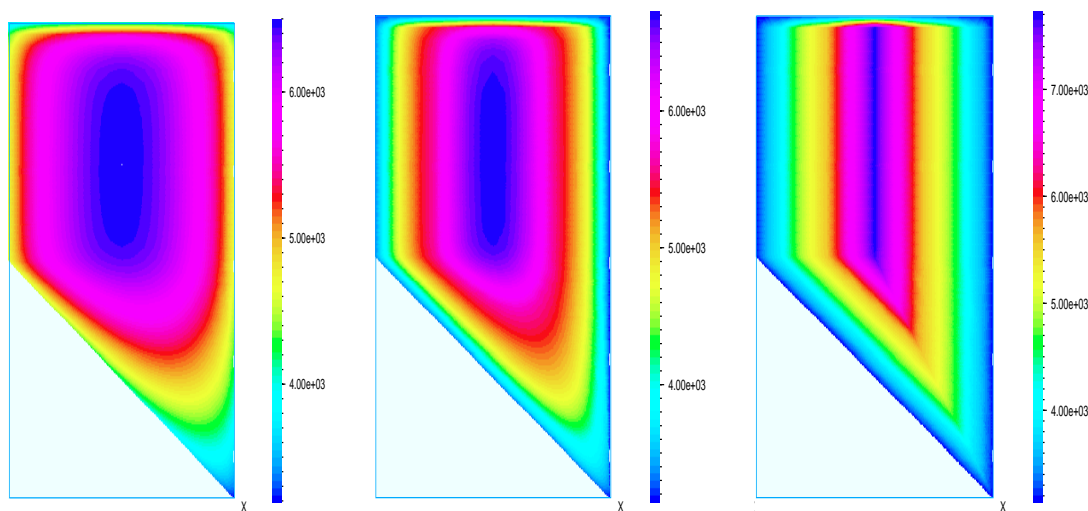


Fig. 6a

Fig. 6b

Fig 6c

In summary, the extended atomic data tables capture the majority of the effects of radiation interactions without the need to perform computationally costly detailed line transfer calculations. The effective optical depth,  $\tau_{\text{eff}}$ , allows using these tables in multidimensional geometries. The extended data tables are available from the authors and should be used for modelling optically thick edge plasmas.

**Acknowledgements** This work was performed under the auspices of the U.S. Department of Energy, by the University of California, Lawrence Livermore National Laboratory under contract W-7405-ENG-48.

#### References

1. M.L. Adams, Ph.D. Thesis, MIT, Cambridge, MA, 2003.
2. H.A. Scott and M.L. Adams, *Contributions to Plasma Physics* 44, pp 51-56 (2004).